States of Molecular Associates in Binary Mixtures of Acetic Acid with Protic and Aprotic Polar Solvents: A Raman Spectroscopic Study †

ARTICLE *in* THE JOURNAL OF PHYSICAL CHEMISTRY A · APRIL 2002

Impact Factor: 2.69 · DOI: 10.1021/jp012606v

2 AUTHORS, INCLUDING:

Nobuyuki Nishi
Faculdade de Odontologia do Recife
164 PUBLICATIONS **3,591** CITATIONS

SEE PROFILE

States of Molecular Associates in Binary Mixtures of Acetic Acid with Protic and Aprotic Polar Solvents: A Raman Spectroscopic Study†

Takakazu Nakabayashi and Nobuyuki Nishi*

Department of Electronic Structure, Institute for Molecular Science, Myodaiji, Okazaki 444-8585, Japan

Received: July 11, 2001; In Final Form: October 23, 2001

The local structures of acetic acid in protic and aprotic polar solvents have been studied by Raman spectroscopy and ab initio calculations with the self-consistent reaction field (SCRF) method. As acetic acid is diluted in water, the C═O stretching Raman band of acetic acid becomes broader and shows a higher wavenumber shift from 1666 to 1710 cm^{-1}, which arises from the generation of acetic acid microphases. In the region of $0.001 \leq \chi_A$ (acetic acid mole fraction) ≤ 0.2, both the peak position and the bandwidth of the C═O band are hardly changed, indicating that the acetic acid microphases exist even in the diluted solution at $\chi_A = 0.001$. In alcohols (methanol, 1-butanol, and 1-hexanol), the spectral changes in the C═O band with the dilution are almost the same as those observed in water, suggesting that the same acetic acid microphases are formed in the alcohol solutions at $\chi_A \geq 0.001$. In acetonitrile, however, the spectral changes are apparently different from those in the protic solvents: two higher wavenumber C═O bands at 1725 and 1754 cm^{-1} appear in the region of $0.001 \leq \chi_A \leq 0.3$. From the ab initio SCRF calculations, we assign the 1725 and 1754 cm^{-1} bands to the cyclic dimer consisting of acetic acid and acetonitrile monomers and to the noncomplexed acetic acid monomer, respectively. Such two bands are also observed in other nitriles and ethers, suggesting that the monomeric molecules are preferentially formed in aprotic polar solvents. From these results, it is concluded that binary solutions of acetic acid and the protic solvents do not get homogeneously mixed even in the low acid concentration region of $\chi_A \geq 0.001$, while homogeneously mixed states at molecular levels occur in binary solutions of acetic acid and the aprotic polar solvents when the acetic acid mole fraction is small. We discuss the empirical rules about the mixture states at molecular levels on the basis of the results obtained.

1. Introduction

The structures and dynamics of pure and mixed liquids at molecular levels have received much attention over the past three decades and still remain a major subject of growing interest in chemical physics. If there is no phase boundary in a binary solution, two constituent solvents have been thought to mix with each other homogeneously. However, it does not follow from this that the mixture is also mixed homogeneously even at a molecular level. Although molecules in a liquid have been considered to move almost randomly with the thermal energy *kT*, some liquid structures have been proposed in both protic[1−4] and aprotic[5] polar solvents.

The purpose of this study is to understand the local structures of acetic acid in the liquid and solution states at the molecular scale. Since acetic acid has four hydrogen-donor sites (a hydroxyl hydrogen and three methyl hydrogens) and two acceptor sites (a hydroxyl oxygen and a carboxyl oxygen) in a molecule, various kinds of acetic acid associates can be expected in various situations. In the vapor phase, acetic acid forms a centrosymmetric cyclic dimer containing two O−H···O═C hydrogen bonds at temperatures below 150 °C (Figure 1).[6,7] These hydrogen bonds are known to be quite strong: Chao and Zwolinski have reported the enthalpy of association to be −14.92 kcal/mol.[8] Some other carboxylic acids also form such cyclic dimers in the gas phase.[6,9,10] In the crystalline state, on the other hand, acetic acid exists in infinite chains that involve

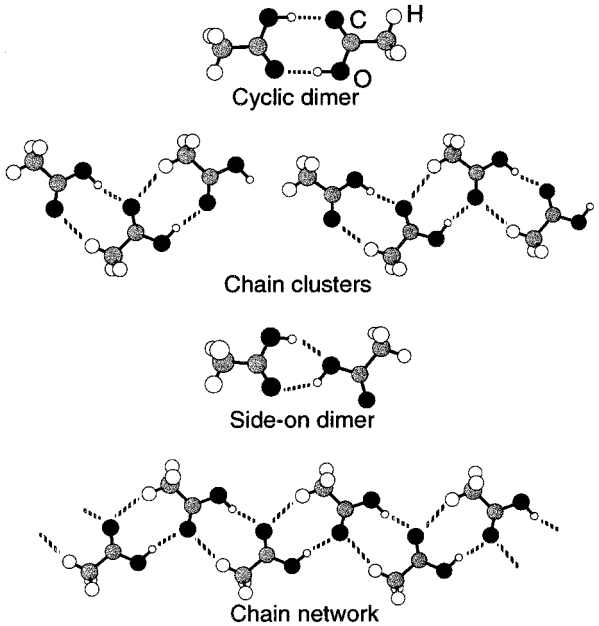

Figure 1. Structures of acetic acid clusters in various situations.

C−H···O═C as well as O−H···O═C hydrogen bonds as depicted in Figure 1.[11−13] Stacking of the chains and the interactions between the stacks result in the crystal structure of acetic acid. From ab initio molecular orbital (MO) calculations on large acetic acid clusters, Turi and Dannenberg have indicated that cooperativity for interactions between different directions

† Part of the special issue "Mitsuo Tasumi Festschrift".

* To whom correspondence should be addressed. Fax: +81-564-54-2254. E-mail: nishi@ims.ac.jp.

10.1021/jp012606v CCC: $22.00
Published on Web 01/09/2002

as well as within each of the three directions is of great importance in the stabilization of the chain structures in the solid.[14] Formic acid also exists in similar polymer chains in the crystalline state,[15] but other carboxylic acids, such as propionic and monofluoroacetic acids, crystallize as associated cyclic dimers similar to those that exist in the gas phase.[16−19]

In the pure liquid state, neutron diffraction experiments have suggested that the associated cyclic dimer structure yields a good description of the liquid structure of acetic acid.[20] Intermolecular and intramolecular Raman bands of liquid acetic acid have been observed and assigned to vibrational modes of the cyclic dimer.[21,22] Their assignments, however, were based on the assumption that the cyclic dimer is the predominant structure in the liquid.[21,22] Theoretically, Monte Carlo simulations have suggested that liquid acetic acid is mainly composed of the hydrogen-bonded chains and not the cyclic dimer.[23] Recently we have observed the Raman spectra of acetic acid in a wide wavenumber region of 15−3700 cm^{-1} at various temperatures.[24,25] By performing ab initio MO calculations on the Raman spectra of seven acetic acid clusters, we have indicated that liquid acetic acid consists primarily of a variety of sizes of chain clusters as the fragments of the crystalline networks (Figure 1).[24,25] This suggests that the cooperativity for hydrogen-bonding interactions among acetic acid molecules is one of the vital factors governing the local structures of liquid acetic acid.

The states of acetic acid associates in aqueous solutions have also been studied by various methods.[24,26−34] Kaatze et al. have found that acetic acid−water mixtures show two dielectric relaxation terms attributed to the presence of two microphases: one is the water rich phase, and the other one is acetic acid.[32] The mass spectrometric analyses of clusters generated through adiabatic expansion of liquid droplets in a vacuum have also indicated that the acetic acid molecules preferentially form their aggregates in binary solutions of acetic acid and water.[33] Recently we have observed the Raman spectra of acetic acid−water mixtures and suggested that a side-on dimer, which is depicted in Figure 1, or a microphase in which this dimer structure is an elementary unit is most likely for acetic acid at high acetic acid concentrations in aqueous solutions.[24,34] This means that the dimer structure with a large electric dipole moment is more stable than the cyclic dimer with a null dipole moment in aqueous solutions, although the cyclic dimer is quite stable in the gas phase.

Theoretical calculations in the presence of solvents have also provided a wealth of information on molecular properties in solution states. Among various methods, self-consistent reaction field (SCRF) methods have been most frequently used in interpreting solvent effects on a solute electronic structure.[35−38] In these methods, the solute occupies a cavity surrounded by the dielectric continuous solvent. A dipole and/or multipole in the solute will induce a reaction field, which in turn will act to electrostatically stabilize the solute. These methods have an advantage of allowing the geometry and dipole moment of the solute to be adjusted to reflect the interaction with the continuous medium, although they cannot treat local solute−solvent interactions such as hydrogen bonds in water. The reference interaction site model self-consistent-field (RISM-SCF) method maintains the molecular aspects of solvents and thus has an advantage of describing specific interactions.[39−41] Quite recently we have applied the RISM-SCF method to investigate the acetic acid dimers in aqueous solutions and found the marked stabilization due to solvation in the side-on dimer (Figure 1).[41]

What should be discussed next is whether the acetic acid microphases also exist in other solvents or not. If the cooperativity for interactions among acetic acid molecules is of great importance in the stabilization of acetic acid, the microphases should also exist in other solvents, while if the local interaction between two acetic acid molecules is essential, acetic acid should form the cyclic configuration in Figure 1. In this study, we report the Raman spectra of acetic acid in aprotic as well as protic polar solvents with varying temperatures and mole fractions of acetic acid (χ_A) from 1 to 0.001. For the estimation of the associated structures in aprotic polar solvents, ab initio MO and density functional theory (DFT) calculations on acetic acid cluster species are also performed with the SCRF method. From the results obtained and the previous reports about other binary mixtures, we discuss the empirical rules about the mixture states at molecular levels.

2. Materials and Methods

High-purity water is prepared by a Puric-Z water purifier (Organo Co. Ltd.). Solvents of special reagent grade are purchased from Wako Pure Chemical Industries and used without further purification. Sample solutions are sealed in 6 mm (i.d.) Pyrex glass tubes. Silicon rubber heaters wound on the sealed glass tube are used for the temperature control. The temperature of the sample is monitored by a thermocouple placed ∼1 mm down from the laser point. Raman spectra are obtained with a Q-switched intracavity frequency doubled Nd:YLF laser (Quantronix, 527DP-H, wavelength 527 nm, repetition rate 1 kHz, average power 15 W, pulse duration 150 ns). The average power of the exciting light is ∼5 mW at the sample. The 90°-scattered Raman signal is collected and dispersed by a single spectrograph (JOBIN YVON-SPEX, 500MS) and detected by a CCD detector (Princeton Instruments, LN/CCD-1340PB, 1340 × 400 pixels). The unshifted scattered light is rejected with a holographic notch filter (Kaiser Optical Systems) placed in front of the entrance slit of the spectrograph. The spectral slit width is ∼7 cm^{-1}. The incident laser is linearly polarized, and neither a polarizer nor a polarization scrambler is used to keep the throughput of the spectrometer as high as possible. Polarization dependence of the sensitivity of the spectrometer is separately examined by using the Raman bands of carbon tetrachloride and cyclohexane and is found to be less than 10%. Emission lines from a neon lamp are used to calibrate the Raman shifts. The experimental errors for the absolute Raman wavenumbers are estimated to be ±1.5 cm^{-1}.

In the C═O stretching band region of 1600−1800 cm^{-1}, the Raman spectra reported here are the difference spectra obtained by subtracting the pure solvent spectrum from that of the binary mixture. No strong Raman intensities due to the treated solvents are observed in this region except propylene carbonate and *N*,*N*-dimethylformamide. The C═O stretching Raman band of propylene carbonate at 1782 cm^{-1} and that of *N*,*N*-dimethylformamide at 1660 cm^{-1} are located near that of acetic acid. In this study, therefore, the difference spectra in these solvents are shown except the regions around the solvent C═O stretching bands. In each experiment, the peak position of the C═O band of neat acetic acid is confirmed to be at the same pixel number of the CCD camera. Thus, the errors for the relative wavenumbers among the C═O bands are estimated to be ±0.3 cm^{-1}.

For measurements in the low-wavenumber region of 14−380 cm^{-1}, the Raman-scattered light at 90° is analyzed by an NR-1800 Raman spectrometer (JASCO) equipped with a triple monochromator and a thermoelectrically cooled photomultiplier tube (Hamamatsu Photonics R943-02). The Raman spectra are excited with the 514.527 nm line from an Ar^+ ion laser (NEC), the average power of which is ∼150 mW at the sample.[24]

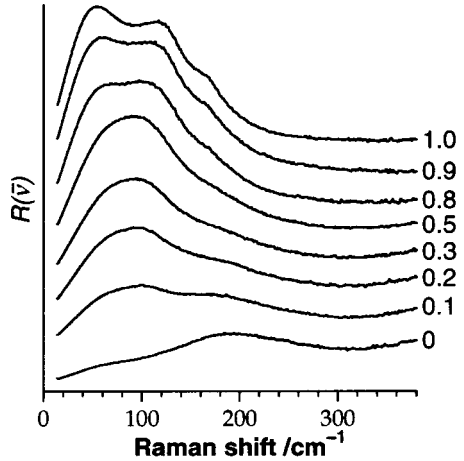

Figure 2. $R(\bar{\nu})$ spectra of acetic acid and water binary solutions in the region of 14−380 cm^{-1} at different mixing ratios. The mole fraction of acetic acid is given on the right of each spectrum.

Ab initio MO and DFT calculations are performed by using the Gaussian 98 program package[42] on an NEC SX-5 supercomputer at the Research Center for Computational Science, Okazaki, Japan. The Hartree−Fock (HF) level method is employed in the ab initio MO calculations. DFT calculations are performed by Becke's three-parameter hybrid method[43] with the Lee−Yang−Parr correlation (B3LYP).[44,45] The 6-311++G** basis set is used throughout.

The acetic acid molecules are optimized to have a C_s plane containing the heavy atoms and a methyl hydrogen at the side of the C═O group. The other two methyl hydrogens are located symmetrically above and under the carboxylic plane. The acetonitrile monomers and the cluster species are also optimized with C_s symmetry.

We apply the SCRF model that makes use of a spherical cavity and considers the solute dipole. The cavity radii employed in the SCRF calculations are determined by means of the VOLUME keyword in the Gaussian 98 program, so that they are consistent with the molecular volumes of the optimized structures.

3. Results and Discussion

3.1. Binary Mixtures of Acetic Acid with Protic Solvents. Figure 2 shows the low-frequency Raman spectra of binary solutions of acetic acid and water with varying mole fractions of acetic acid. Those spectra are presented as a function of the so-called $R(\bar{\nu})$, which is calculated as $R(\bar{\nu}) \propto I(\bar{\nu})\bar{\nu}[1 - \exp(-h\bar{\nu}/kT)]$, where $I(\bar{\nu})$ stands for the Raman intensity in the usual sense and $\bar{\nu}$ is the Raman wavenumber shift of the scattered light. The $R(\bar{\nu})$ representation provides the corrected Raman intensity that is directly proportional to the sum of the squares of the polarizability derivatives with respect to normal coordinates. It has the practical advantage of removing the intensity of the exciting laser line. As shown in the previous studies,[24,34] the $R(\bar{\nu})$ spectra of the binary solutions cannot be decomposed into linear combinations of the $R(\bar{\nu})$ spectra of pure water and pure acetic acid. However, the spectra are satisfactorily reproduced by linear combinations of the pure acetic acid spectrum ($\chi_A = 1.0$) and that of the mixture at $\chi_A = 0.5$ in the high acid concentration region ($0.5 \leq \chi_A \leq 1$) and by linear combinations of the pure water spectrum ($\chi_A = 0$) and that of the mixture at $\chi_A = 0.5$ in the low acid concentration region ($0 \leq \chi_A \leq 0.5$). The $R(\bar{\nu})$ spectrum of the diluted mixture at $\chi_A = 0.015$ was also reproduced by a linear combination of the spectra of pure water and the 1:1 mixture.[34] These results indicate that the molecular associates in the binary solutions are quite different from those in the pure liquid states. From comparison between the observed and the ab initio MO calculated Raman spectra, the mixture spectrum at $\chi_A = 0.5$ was found to mainly arise from the side-on dimer acetic acid aggregates and not acetic acid−water complexes.[34]

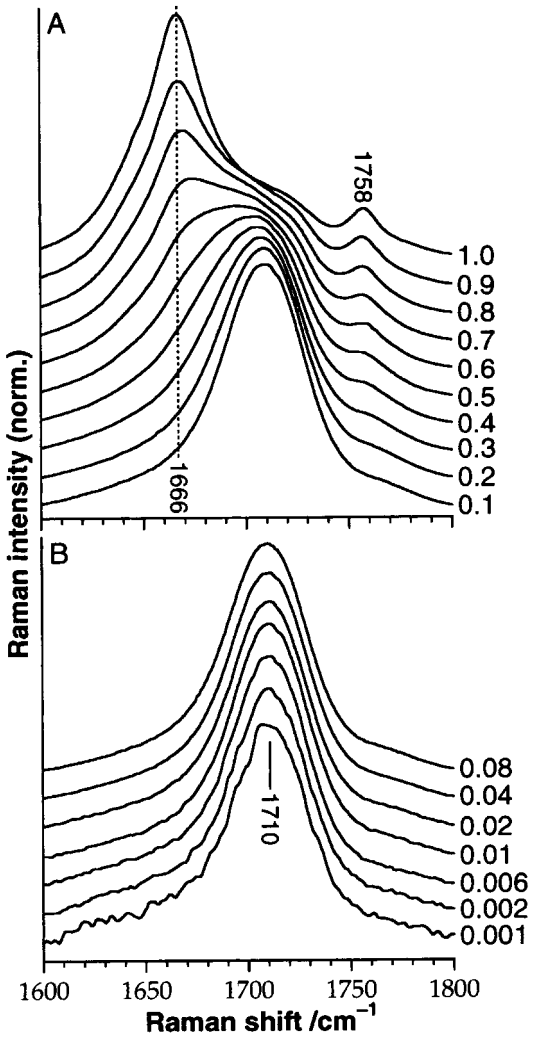

Figure 3. Raman spectra of acetic acid and water binary solutions in the C═O stretching region of 1600−1800 cm^{-1} at different mixing ratios. The mole fraction of acetic acid is given on the right of each spectrum. The intensity scale is normalized for the integrated intensities of the respective spectra in the 1600−1800 cm^{-1} region. Key: A, high acetic acid concentration region; B, low acetic acid concentration region.

The mixing ratio dependence of the Raman spectra of acetic acid and water mixtures in the C═O stretching band region is shown in Figure 3. The intensity scale is normalized for the integrated intensities of the respective spectra in the region of 1600−1800 cm^{-1}. As mentioned above, these spectra are the difference spectra obtained by subtracting the pure water spectrum from the binary mixture one. In the pure acetic acid spectrum ($\chi_A = 1$), the prominent Raman band at ~1666 cm^{-1} can be ascribed to the strongly hydrogen-bonded C═O groups of the long-chain clusters as the fragments of the crystalline networks.[25] The asymmetric components in the region of 1700−1740 cm^{-1} are assigned to the weakly hydrogen-bonded C═O groups of the long- and short-chain species.[25] A weak band at ~1758 cm^{-1} in the pure acetic acid spectrum is considered to be a combination of two intramolecular modes and/or the weakly hydrogen-bonded C═O groups of the chain clusters.

The C═O stretching band of acetic acid has been known to be strongly affected by surroundings.[30,31,34] As is clearly shown in Figure 3, the prominent C═O stretching band broadens and shifts to a higher wavenumber with the addition of water into acetic acid at $\chi_A \geq 0.2$. In the solutions from $\chi_A = 0.2$ to 0.02, slight narrowing of the C═O band is observed, though its peak position remains almost unchanged at ~1710 cm^{-1}. Neither the peak position nor the bandwidth is changed in the low acid concentration region of $0.001 \leq \chi_A \leq 0.02$. From the low-frequency Raman results mentioned above, the broad 1710 cm^{-1} band in the mixture spectra around $\chi_A = 0.2$ can be ascribable to the C═O groups of the acetic acid aggregates in which the side-on dimer structure is an elementary unit. The mass spectra of clusters generated from liquid droplets have also suggested that the acetic acid molecules preferentially form their aggregates in acetic acid−water binary solutions at $\chi_A \sim 0.09$.[33] Since the peak position at 1710 cm^{-1} remains unchanged even in the diluted solution at $\chi_A = 0.001$, it can be concluded that the side-on dimer acetic acid microphases exist in this low acid concentration region. This indicates that binary solutions of acetic acid and water exhibit heterogeneous distributions of the constituent solvent molecules at $\chi_A \geq 0.001$. The low-frequency Raman spectrum of the mixture at $\chi_A = 0.015$ is reproduced by a linear combination of the pure water spectrum and the 1:1 mixture one, the latter of which arises mainly from the side-on dimer aggregates.[34] This result is in accord with the above conclusion.

Figure 4 shows the Raman spectra of binary solutions of acetic acid and methanol with varying mixing ratios in the C═O stretching region. The intensity scale is normalized for the integrated intensities of the respective spectra in the region of 1600−1800 cm^{-1}. Concentration dependence of the spectra of the acetic acid and methanol mixtures is similar to that of the spectra of the acetic acid and water mixtures in Figure 3, although the bandwidth of the C═O stretching band is narrower in methanol than the width in water. With decreasing acetic acid concentration from $\chi_A = 1$ to 0.2, the C═O band shifts to a higher wavenumber and only slight narrowing is observed in the region of $\chi_A = 0.2-0.02$. No concentration dependence of the spectral shape is seen in $0.001 \leq \chi_A \leq 0.02$. It is noted in Figure 4 that the peak position of the C═O band at ~1711 cm^{-1} in methanol is almost the same as that of the C═O band in water. Such a mixing ratio dependence of the C═O band suggests that the acetic acid molecules in methanol also form the side-on dimer aggregates that exist even in the diluted solution at $\chi_A = 0.001$. The broad feature of the low-frequency Raman spectrum of the acetic acid and water mixture at $\chi_A = 0.3$ is similar to that of the spectrum of the acetic acid and methanol mixture at the same mole fraction of acetic acid.[34] This behavior is explained when the side-on dimer aggregates dominate the spectral feature of the acetic acid and methanol mixture at $\chi_A = 0.3$. Figure 5 compares the C═O stretching Raman bands of binary solutions of acetic acid and protic solvents at $\chi_A = 0.006$. In any protic solvents used, no mixing ratio dependence of the spectral shape is observed around this mole fraction. In Figure 5, the peak position of the C═O stretching band is hardly affected by the protic solvent added. Furthermore, as shown in the case of methanol in Figure 4, the observed spectral changes of the acetic acid and alcohol mixtures are almost the same as that of the acetic acid and water mixture. These results lead us to a conclusion that binary solutions of acetic acid and the protic solvents at $\chi_A \geq 0.001$ consist of the two microphases: an acetic acid rich phase and a protic solvent rich phase. Phase separations at molecular levels occur in binary solutions of acetic acid and the protic solvents at $\chi_A \geq 0.001$.

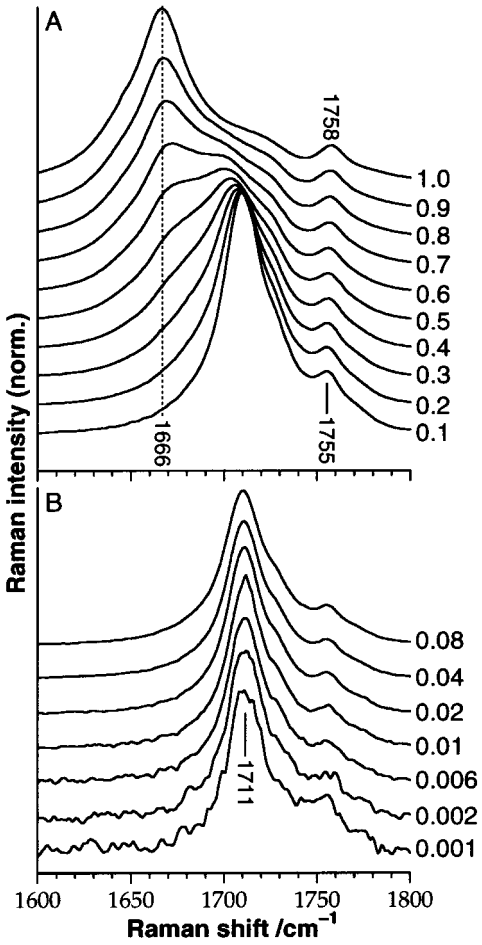

Figure 4. Raman spectra of acetic acid and methanol binary solutions in the C═O stretching region of 1600−1800 cm^{-1} at different mixing ratios. The mole fraction of acetic acid is given on the right of each spectrum. The intensity scale is normalized for the integrated intensities of the respective spectra in the 1600−1800 cm^{-1} region. Key: A, high acetic acid concentration region; B, low acetic acid concentration region.

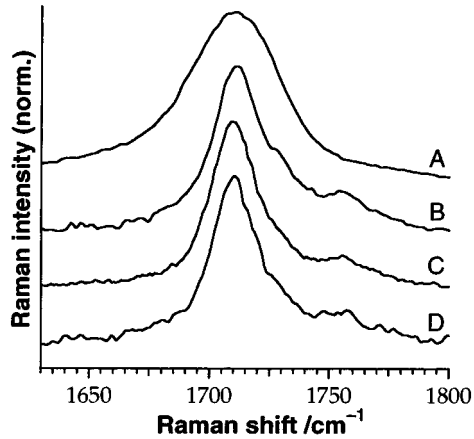

Figure 5. Raman spectra of acetic acid in the C═O stretching region of 1630−1800 cm^{-1} in water (A), methanol (B), 1-butanol (C), and 1-hexanol (D). The intensity of each spectrum is normalized by reference to the peak intensity of the prominent C═O stretching band. The mole fraction of acetic acid is 0.006.

The weak band at ~1755 cm^{-1} is seen in the diluted alcohol solutions in Figure 5, although such a weak band seems to disappear at $\chi_A \leq 0.1$ in water. This behavior may be interesting; however, in this study, we cannot determine whether this weak

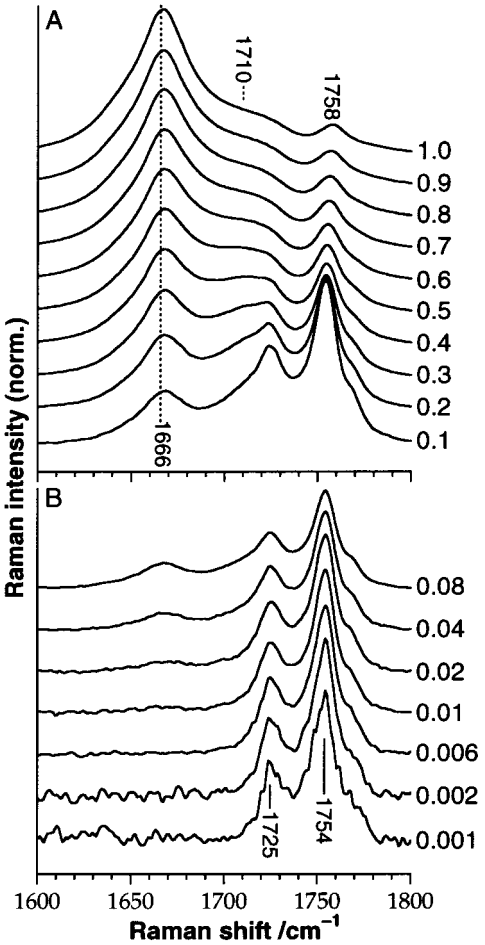

Figure 6. Raman spectra of acetic acid and acetonitrile binary solutions in the C═O stretching region of 1600−1800 cm^{-1} at different mixing ratios. The mole fraction of acetic acid is given on the right of each spectrum. The intensity scale is normalized for the integrated intensities of the respective spectra in the 1600−1800 cm^{-1} region. Key: A, high acetic acid concentration region; B, low acetic acid concentration region.

band is attributed to a combination of two intramolecular modes or to the weakly hydrogen-bonded C═O groups of the acetic acid clusters. More elaborate Raman measurements in a wider wavenumber region are needed for the assignment of this band.

3.2. Binary Mixtures of Acetic Acid with Acetonitrile. Acetonitrile is an aprotic polar solvent unlike water and alcohol and possesses a lone pair acting as a Lewis base. Figure 6 shows the Raman spectra of acetic acid and acetonitrile mixtures with varying mixing ratios in the C═O stretching band region. The intensity scale is normalized for the integrated intensities of the respective spectra in the region of 1600−1800 cm^{-1}. Apparently, mixing ratio dependence of the spectra of acetic acid and acetonitrile mixtures is different from those of the spectra of binary solutions of acetic acid and the protic solvents in Figures 4 and 5. In the high acid concentration region of $0.3 \leq \chi_A \leq 1$, dilution of acetic acid first increases the intensities of the asymmetric bands in the 1700−1740 cm^{-1} region relative to that of the prominent C═O stretching band at 1666 cm^{-1}. The relative intensity of the weak band around 1758 cm^{-1} also becomes larger. In the region from $\chi_A = 0.3$ to 0.006, two Raman bands appear at ∼1725 and ∼1754 cm^{-1}, and their fractions in the total integrated intensity in the 1600−1800 cm^{-1} region become larger. As for the 1666 cm^{-1} band, its fraction in the total integrated intensity monotonically decreases. In the region of $0.001 \leq \chi_A \leq 0.006$, the 1666 cm^{-1} band completely disappears and no spectral change is observed within the

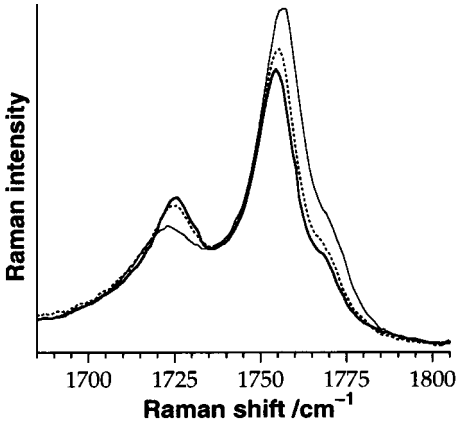

Figure 7. Raman spectra of acetic acid and acetonitrile binary solutions in the C═O stretching region of 1685−1805 cm^{-1} at different temperatures. The mole fraction of acetic acid is 0.01. Key: thick-solid trace, 292 K; dotted trace, 325 K; thin-solid trace, 340 K.

experimental accuracy. The peak position of the 1666 cm^{-1} band is almost independent of the acid concentration, and those of the 1725 and 1754 cm^{-1} bands also remain unchanged in the $0.001 \leq \chi_A \leq 0.3$ region. The intensity of the 1725 cm^{-1} band relative to that of the 1754 cm^{-1} band hardly changes in the $0.001 \leq \chi_A \leq 0.1$ region.

Temperature dependence of the 1725 and 1754 cm^{-1} bands of the acetic acid and acetonitrile mixture at $\chi_A = 0.01$ is shown in Figure 7. Spectral changes with the temperature are clearly observed in both the two bands. As the temperature grows, the 1725 cm^{-1} band slightly broadens and shifts to a lower wavenumber, while the 1754 cm^{-1} band shifts to a higher wavenumber and its bandwidth remains almost constant. The intensity of the 1754 cm^{-1} band relative to that of the 1725 cm^{-1} band becomes larger with the temperature. Such spectral changes with the concentration and temperature should reflect the local structures of binary solutions of acetic acid and acetonitrile.

As mentioned above, we have ascribed the 1666 cm^{-1} band in the liquid acetic acid spectrum to the strongly hydrogen-bonded C═O groups of the long-chain clusters and the asymmetric components in the 1700−1740 cm^{-1} region to the weakly hydrogen-bonded C═O groups of the long- and short-chain species.[25] From the ab initio MO calculations for the C═O stretching modes of the chain clusters, it has also been suggested that the prominent C═O stretching band shifts to a higher wavenumber with decreasing aggregate size.[25] Thus, in the solutions with $0.3 \leq \chi_A \leq 1$, as seen in Figure 6, the first increase in the intensities of the asymmetric components in the 1700−1740 cm^{-1} region relative to that of the 1666 cm^{-1} band may be related to the dissociation of the long-chain clusters into the short-chain clusters and the monomer.

In the $0.001 \leq \chi_A \leq 0.3$ region, the 1725 and 1754 cm^{-1} bands cannot be assigned to the C═O stretching bands of the monomer and the cluster consisting of a few acetic acid molecules, respectively. This is because the relative intensity between the two bands is almost independent of the acid concentration. The marked change in the relative intensity with the temperature indicates that the two bands cannot arise from two different modes of the same acetic acid cluster. From these considerations, it is conceivable that the two bands appeared with increasing dilution arise from two types of acetic acid monomers in different environment. The hetero dimers consisting of acetic acid and acetonitrile monomers and the uncomplexed acetic acid monomer can be given as examples. This result is in agreement with the mass spectrum of a cluster beam

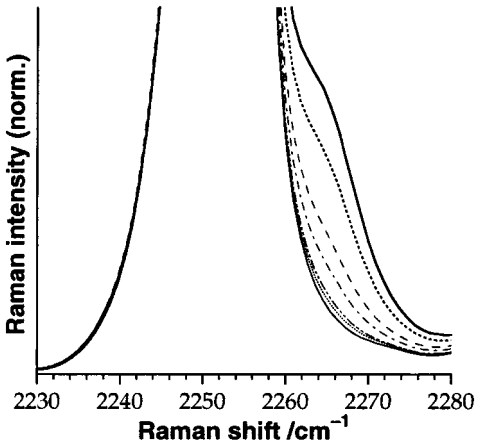

Figure 8. Raman spectra of acetic acid and acetonitrile binary solutions in the C≡N stretching region of 2230−2280 cm^{-1} at different mixing ratios. The enlargements of the lower parts of the C≡N stretching bands are shown, although the intensity of each spectrum is normalized by reference to the peak intensity of the C≡N stretching band at 2253 cm^{-1}. Key: thick-solid trace, $\chi_A = 0.3$; thick-dotted trace, 0.2; broken trace, 0.08; dot−dashed trace, 0.04; dot−dot−dashed trace, 0.01; dotted trace, 0.006; thin-solid trace, 0 (pure acetonitrile).

generated from an acetic acid and acetonitrile mixture (molar ratio 1:10), in which large acetic acid clusters are not observed except for the presence of a small amount of acetic acid dimer species.[33] The monomer species contributing to the 1754 cm^{-1} band should be higher in total energy than that contributing to the 1725 cm^{-1} band, since the intensity of the 1754 cm^{-1} band relative to that of the 1725 cm^{-1} band increases with the temperature.

The existence of acetic acid−acetonitrile complexes is confirmed from the measurements of the Raman spectra in the C≡N stretching band region.[46,47] In Figure 8, concentration dependence of the Raman spectra of acetic acid−acetonitrile mixtures in the C≡N stretching region is shown. The subtraction of the acetonitrile-only spectrum has not been carried out in this figure. The enlargements of the lower parts of the C≡N stretching bands are shown, although the intensity scale is normalized for the peak intensities of the respective spectra. In the pure acetonitrile spectrum ($\chi_A = 1$), the strong C≡N band is observed at ∼2253 cm^{-1}. With the addition of acetic acid into acetonitrile, asymmetric components appear at higher wavenumbers, while no marked spectral changes are observed in the lower wavenumber region. Such high-wavenumber components have been observed in other protic solvent−acetonitrile mixtures and considered to arise from complexes of acetonitrile and protic solvents.[5,46−50] Hence the result in Figure 8 can also be ascribed to acetic acid−acetonitrile associates. The higher wavenumber components are clearly seen even in the diluted solution at $\chi_A = 0.006$ in Figure 8. Since only the 1725 and 1754 cm^{-1} bands are observed in the spectrum of this diluted solution in the C═O stretching band region (Figure 6), it can be said that the acetic acid−acetonitrile complexes contribute to the intensities of the two higher wavenumber C═O bands in the diluted acetonitrile solutions.

3.3. Ab Initio Calculations on Monomer and Cluster Species in the Gaseous Phase and in Acetonitrile. To further discuss the existence of two different types of acetic acid monomers in acetonitrile, ab initio MO and DFT calculations on acetic acid and acetonitrile dimers and the respective monomers are carried out with the SCRF method. Ab initio calculations have been widely used to examine the energies and the vibrational spectra of neutral monomers and clusters.[14,25,37,38,47] The SCRF method has also been shown to be useful for the

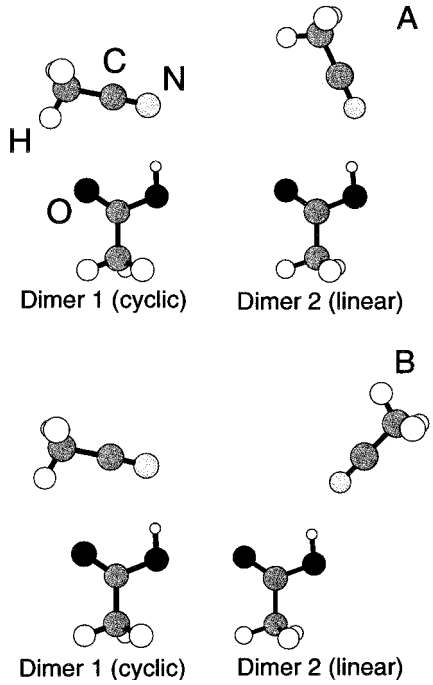

Figure 9. Optimized geometries of acetic acid and acetonitrile dimers in the gaseous phase (A) and in acetonitrile (B) at the B3LYP/6-311++G** level.

analyses of solvent effects on vibrational wavenumbers.[37,38] The application of the SCRF method to the acetonitrile monomer means that the molecular properties of the acetonitrile monomer in acetonitrile are calculated. As shown in Figure 9A, two kinds of dimers consisting of acetic acid and acetonitrile monomers are optimized in the gas phase at the B3LYP/6-311++G** level. Dimer 1 forms a cyclic structure containing two intermolecular interactions: one O−H···N≡C and one C═O···H−C interaction, while dimer 2 forms a linear structure involving only one O−H···N≡C interaction. The optimized geometries of these dimers in acetonitrile are shown in Figure 9B. The dielectric constant of acetonitrile is assumed to be 36.64. The marked geometrical change on going from the gas phase to the acetonitrile solution is seen in dimer 2: the C≡N bond of acetonitrile and the C═O bond of acetic acid are on the same side in the gas phase and on the opposite side in acetonitrile. As discussed later, this behavior can be attributed to the enhancement of a solute−solvent interaction resulting in the greater stabilization of dimer 2 in the solution. The ab initio MO calculations at the HF/6-311++G** level show almost the same results.

Table 1 shows the calculated total and binding energies of these dimers in the gas phase and in acetonitrile at the B3LYP/6-311++G** level. The corrected energies for zero-point vibrational energies (ZPVE) and the total energies of the acetic acid and acetonitrile monomers are also shown in this table. In the gas phase, the energy difference between dimer 1 and dimer 2 is estimated to be small: dimer 1 is more stable than dimer 2 by 0.55 kcal/mol. The C═O···H−C interaction contributes to the stabilization in the cyclic structure. On the other hand, in acetonitrile, dimer 2 becomes more stable by 2.50 kcal/mol than dimer 1, indicating that the interaction between dimer 2 and the continuous solvent is much stronger than that between dimer 1 and the solvent. It is noticeable that the acetic acid and acetonitrile monomers also obtain stabilization in acetonitrile: 0.62 and 3.99 kcal/mol, respectively.

Table 2 compares the electric dipole moments calculated in the gas phase and in acetonitrile. All the dipole moments are

TABLE 1: Total and Binding Energies[a] of Acetic Acid and Acetonitrile Monomers and Their Dimers in the Gaseous Phase and in Acetonitrile[b] at the B3LYP/6-311++G Level**

	tot. energy (hartrees)		binding energy[c] (kcal/mol)	
	gas	acetonitrile	gas	acetonitrile
acetic acid monomer	−229.164 826 8	−229.165 821 8		
acetonitrile monomer	−132.796 200 7	−132.802 566 2		
dimer 1	−361.971 740 3	−361.972 987 0	6.72 (5.89)	2.89 (2.07)
dimer 2	−361.970 862 3	−361.976 971 2	6.17 (5.42)	5.39 (4.74)

[a] Binding energy is defined as the difference between the energy of a dimer and the sum of the energies of separated monomer molecules in each state. [b] The cavity radii employed in the SCRF method are 3.40 Å for acetic acid monomer, 3.24 Å for acetonitrile monomer, 4.11 Å for dimer 1, and 4.10 Å for dimer 2. [c] Values in parentheses correspond to ZPVE-corrected binding energies.

TABLE 2: Dipole Moments (in D) of Acetic Acid and Acetonitrile Monomers and Their Dimers in the Gaseous Phase and in Acetonitrile at the B3LYP/6-311++G Level**

	gas	acetonitrile
acetic acid monomer	1.74	2.04
acetonitrile monomer	4.05	4.86
dimer 1	2.56	3.07
dimer 2	4.06	7.73

estimated to become larger on going from the gas phase to the solution. The marked change occurs in the dipole moment of dimer 2: its dipole moment in acetonitrile is about twice as large as that in the gas phase. Such a large increase in the dipole moment enhances the solute−solvent electrostatic interaction and contributes to the greater stabilization in dimer 2. The dipole moment of the acetonitrile monomer also becomes much larger in acetonitrile, which is consistent with the great stabilization in the acetonitrile monomer in the acetonitrile solution mentioned above.

The optimized geometries characteristic of intermolecular interactions in the gas phase are shown in Table 3. The C═O and O−H bond lengths calculated for both the dimers are longer than those for the acetic acid monomer, which indicates that the interaction of an acetic acid with an acetonitrile monomer lengthens these intramolecular bonds. On the other hand, the C≡N bond length of dimer 2 is shorter than that of the acetonitrile monomer. The same behavior is also obtained from the ab initio MO calculations at the HF/6-311++G** level. This result can be considered to arise from the effective transfer of the charge from the C≡N antibonding orbital to the orbital forming the intermolecular bond in the linear configuration.[46,51] Dimer 2 has a shorter H···N distance in the O−H···N≡C bond than dimer 1. This means that the O−H···N≡C interaction in dimer 2 is stronger than that in dimer 1.

The geometries optimized in acetonitrile are also collected in Table 3. As mentioned before, the dipole moments of all the species become larger on going from the gas phase to the acetonitrile solution. In other words, all the dipolar molecules change their geometries to obtain higher stabilization due to the electrostatic interaction with the continuous solvent. Thus, the C═O bond lengths of the acetic acid monomer and dimer 2 become longer in the solution than in the gas phase. The C═O bond length of dimer 1 is, however, shortened by the interaction with the continuous solvent. Since the O···H distance for the C═O···H−C bond of dimer 1 is lengthened in acetonitrile, this opposite behavior can be considered to arise from the decrease in the C═O···H−C intermolecular interaction. Geometrical changes for enlarging the dipole moment make the C═O···H−C distance longer and its intermolecular interaction weaker in acetonitrile. The H···N distances of both the dimers are shortened in the acetonitrile solution, which indicates that the O−H···N≡C interaction becomes stronger in the solution. The change in the H···N distance of dimer 2 is much larger than that in the H···N distance of dimer 1. The C≡N and O−H bond lengths of dimer 2 are calculated to become longer on going from the gas phase to the solution, while those of dimer 1 are calculated to remain almost unchanged. These results indicate that the interaction with the continuous acetonitrile solvent affects the geometry of dimer 2 more than that of dimer 1. Because of the cyclic structure, the dipole moment of dimer 1 is smaller than those of dimer 2 and the acetonitrile monomer. Thus, the interaction between dimer 1 and the solvent cannot become so large, which causes the small change in the geometrical structure of dimer 1. The C≡N bond length of the acetonitrile monomer becomes slightly longer in acetonitrile than in the gas phase.

Calculated wavenumbers of the C═O and C≡N stretching modes are collected in Table 4. The wavenumbers listed are not multiplied by a scale factor. On going from the gas phase to the solution, the C═O stretching modes of the acetic acid monomer and dimer 2 shift to lower wavenumbers and that of dimer 1 shifts to a higher wavenumber. This behavior is in consistent with the result in Table 3 that the C═O bonds of the monomer and dimer 2 are lengthened and that of dimer 1 is shortened by the interaction with the continuous solvent. All the C≡N stretching modes are calculated to shift to lower wavenumbers in the acetonitrile solution. Because of the large low-wavenumber shift of the C≡N mode of the acetonitrile monomer, the C≡N stretching wavenumber of dimer 1 becomes higher than that of the acetonitrile monomer in acetonitrile.

As shown in Table 1, dimer 2 is calculated to obtain the greater stabilization due to solvation than dimer 1 in the acetonitrile solution. However, dimer 2 optimized in acetonitrile has one CH_3 torsional mode with an imaginary wavenumber at the B3LYP/6311++G** and the HF/6311++G** levels, although the wavenumbers of all the modes are real in the gas phase at the same levels. This means that the linear dimer structure becomes a saddle point in the solution. On the other hand, dimer 1 has no imaginary wavenumber in both the phases at the above two levels, indicating that the cyclic structure is calculated to be at the potential energy minimum even in acetonitrile. From these results, it can be concluded that the acetic acid−acetonitrile dimer has the cyclic configuration, not the linear configuration, at the global energy minimum in the acetonitrile solution.

Changes in the solvent temperature cause changes in the dielectric constant of the solvent. In the case of acetonitrile, the dielectric constant decreases with increasing temperature,[52] which means that the solute−solvent electrostatic interaction becomes weaker as the temperature grows. The low-wavenumber shift of the 1725 cm^{-1} band and the high-wavenumber shift of the 1754 cm^{-1} band with the temperature (Figure 7) can be therefore considered to arise from the decrease in the solute−solvent interaction. As mentioned in Table 4, the C═O stretching mode of the cyclic dimer shows a lower wavenumber shift on going from the acetonitrile solution to the gas phase. This is due to the increase in the intermolecular interaction between

TABLE 3: Geometrical Parameters[a,b] of Acetic Acid and Acetonitrile Monomers and Their Dimers in the Gaseous Phase and in Acetonitrile at the B3LYP/6-311++G Level**

	acetic acid monomer		acetonitrile monomer		dimer 1		dimer 2	
	gas	acetonitrile	gas	acetonitrile	gas	acetonitrile	gas	acetonitrile
r(C═O)	1.205	1.208			1.212	1.210	1.210	1.212
r(C≡N)			1.153	1.154	1.153	1.153	1.151	1.152
r(O−H)	0.969	0.969			0.980	0.980	0.982	0.988
r(H···N)[c]					1.988	1.983	1.915	1.873
r(O···H)[d]					2.595	2.628		

[a] Selected geometrical parameters characteristic of intermolecular interactions are shown. [b] In units of angstroms. [c] Intermolecular H···N distance for the O−H···N≡C bond. [d] Intermolecular O···H distance for the C═O···H−C bond.

the constituent monomers. On the other hand, the C═O stretching wavenumber of the noncomplexed acetic acid monomer is calculated to be higher in the gas phase than in the solution. These results indicate that the C═O band of the cyclic dimer shifts to a lower wavenumber and that of the noncomplexed acetic acid monomer shifts to a higher wavenumber as the electrostatic interaction decreases. Therefore, the positional changes in Figure 7 can be explained when the 1725 cm^{-1} band is ascribed to the C═O band of the cyclic dimer and the 1754 cm^{-1} band to that of the noncomplexed acetic acid monomer. The cyclic dimer is calculated to be more stable by 2.89 kcal/mol than the separated monomer molecules in acetonitrile (Table 1). Thus, these assignments are consistent with the intensity change in Figure 7 that the ratio of the intensity of the 1754 cm^{-1} band to that of the 1725 cm^{-1} band increases with the temperature. Because of the small force constants of the intermolecular modes, the broadening of the 1725 cm^{-1} band can be thought to arise from the distribution of the cyclic structures with different intermolecular distances at high temperatures. In acetonitrile, the C≡N stretching wavenumber of the cyclic dimer is calculated to be higher than that of the free acetonitrile monomer, which is in agreement with the spectra shown in Figure 8. This result also suggests that, in the case of acetic acid and acetonitrile mixtures, the high-wavenumber shift of the C≡N band due to the complex formation mainly arises from the large low-wavenumber shift of the C≡N band of the noncomplexed acetonitrile monomer in acetonitrile and not the charge transfer from the C≡N antibonding orbital in the complex.[46,51]

In consequence, from the comparison of the experimental and the theoretical results, we assign the 1725 cm^{-1} band to the C═O stretching band of the cyclic dimer consisting of acetic acid and acetonitrile monomers (Figure 9) and the 1754 cm^{-1} band to that of the noncomplexed acetic acid monomer. The acetic acid molecules are found to be preferentially distributed as the monomer species in acetonitrile.

3.4. Binary Mixtures of Acetic Acid with Aprotic Polar Solvents. Figure 10 compares the C═O stretching Raman bands of binary solutions of acetic acid and aprotic polar solvents at $\chi_A = 0.08$. Some physical properties of the solvents and the observed peak wavenumbers are collected in Table 5. The spectra in this figure can be roughly classified in two groups according to the spectral shape. Two higher wavenumber bands in acetonitrile (A) are also seen in propionitrile (B), 1,4-dioxane (C), tetrahydrofuran (D), and propylene carbonate (E), while one prominent band with a higher wavenumber asymmetric shape is observed in *N*,*N*-dimethylformamide (F) and dimethyl sulfoxide (G). This tendency correlates well with Gutmann electron-donor numbers (DN)[53] that are listed in Table 5: two higher wavenumber bands are observed in the solvents with lower DNs, and one prominent band with an asymmetric shape is seen in the solvents with higher DNs. On the other hand, dielectric constants have no correlation with the spectral shapes: the dielectric constant of propylene carbonate is the largest and that of 1,4-dioxane is the smallest among those of the solvents used, while the two higher wavenumber bands are observed in both the solvents.

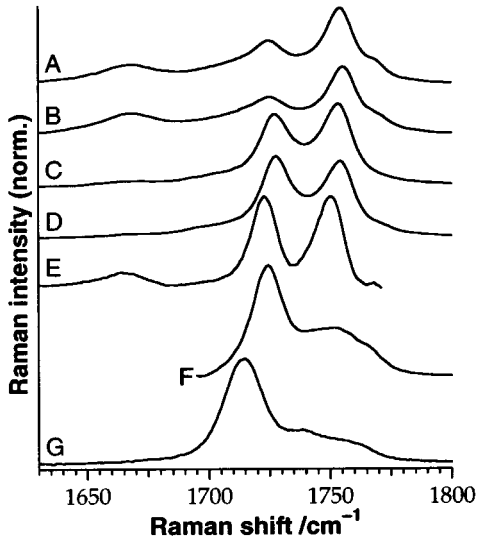

Figure 10. Raman spectra of acetic acid in the C═O stretching region of 1630−1800 cm^{-1} in acetonitrile (A), propionitrile (B), 1,4-dioxane (C), tetrahydrofuran (D), propylene carbonate (E), *N*,*N*-dimethylformamide (F), and dimethyl sulfoxide (G). The intensity scale is normalized for the integrated intensities of the respective spectra in the 1630−1800 cm^{-1} region. The mole fraction of acetic acid is 0.08. It has not been possible to obtain reliable difference spectra in the blank regions in E and F because of interference by strong solvent Raman bands.

TABLE 4: C═O and C≡N Stretching Wavenumbers (cm^{-1}) of Acetic Acid and Acetonitrile Monomers and Their Dimers in the Gaseous Phase and in Acetonitrile at the B3LYP/6-311++G Level**

	C═O		C≡N	
	gas	acetonitrile	gas	acetonitrile
acetic acid monomer	1817.6	1795.7		
acetonitrile monomer			2361.9	2347.5
dimer 1	1783.8	1787.3	2356.9	2351.7
dimer 2	1793.9	1772.3	2378.5	2366.9

As discussed in subsection 3.3, the two higher wavenumber bands appeared in acetonitrile can be attributed to the C═O stretching band of the cyclic dimer consisting of acetic acid and acetonitrile monomers and that of the noncomplexed acetic acid monomer. Since no significant differences are seen among the peak positions of the observed two bands in Figure 10A−E, we conclude that the two different types of acetic acid monomers exist not only in acetonitrile but also in other aprotic polar solvents with lower DNs. The Gutmann electron-donor number is one of the empirical parameters measuring an electron-donating property of a solvent.[53] Thus, it can be said

TABLE 5: Properties[a] of Aprotic Polar Solvents Treated and Wavenumbers (cm^{-1}) of Observed C═O Stretching Bands of Acetic Acid

solvent	DN	ϵ	μ	ρ	wavenumber	
acetonitrile	14.1	36.6	3.9	0.0191	1725	1754
propionitrile	16.1	29.7	4.1	0.0142	1725	1755
1,4-dioxane	14.8	2.2	0	0.0117	1727	1753
tetrahydrofuran	20.0	7.5	1.8	0.0123	1728	1754
propylene carbonate	15.1	66.1	4.9	0.0118	1723	1750
N,*N*-dimethylformamide	26.6	38.3	3.8	0.0129	1725	
dimethyl sulfoxide	29.8	47.2	4.0	0.0141	1714	

[a] DN is the Gutmann donor number[53] in kcal mol^{-1}, ϵ is the dielectric constant (dimensionless), μ is the electric dipole moment in D, and ρ is the molar density in mol cm^{-3}. Values are taken from ref 52 except for DN from ref 53.

that acetic acid preferentially exists as monomeric molecules in the aprotic polar solvents with low electron-donating power. This result is consistent with the carbonyl-^{13}C and the ^1H NMR experiments on binary solutions of acetic acid and acetone (DN = 17.0), in which the trends to higher shielding with decreasing acid concentration have been interpreted as the increase in the destruction of hydrogen bonds among acetic acid molecules.[54,55]

The C═O bond of the noncomplexed acetic acid monomer is lengthened by the interaction with the dielectric continuous solvent as shown in Table 3. Thus, it is expected in the dielectric continuum model that the C═O stretching wavenumber of the noncomplexed monomer decreases as the dielectric constant increases (Table 4). By comparing the results in acetonitrile, propionitrile, and propylene carbonate in Table 5, we can find that the highest wavenumber band ascribed to the noncomplexed monomer shifts to a lower wavenumber with increasing dielectric constant. However, the highest wavenumber bands in the ethers (1,4-dioxane and tetrahydrofuran) show wavenumbers lower than that in propionitrile, although the dielectric constants of these ethers are small. Thus, consideration of microscopic solute−solvent interactions may be necessary to fully estimate the stabilization of the acetic acid monomer in 1,4-dioxane and tetrahydrofuran. It is noted in the spectra at $\chi_A = 0.08$ (Figure 10) that the 1666 cm^{-1} band arising from the chain clusters completely disappears in these ethers, while this band still exists in the nitriles and propylene carbonate. This suggests that these ethers have a greater ability to break hydrogen bonds among acetic acid molecules than the nitriles and propylene carbonate.

The spectral features in *N*,*N*-dimethylformamide and dimethyl sulfoxide are apparently different from those in the other aprotic polar solvents shown in Figure 10. Since the wavenumbers of these prominent C═O bands are in the region of 1715−1730 cm^{-1}, the interactions between the acetic acid and the solvent molecules are considered not to be so weak. Thus, it is conceivable that acetic acid−solvent complexes are also formed in the aprotic polar solvents with high electron-donating power. To provide a more definitive conclusion on this point, however, calculations on such complexes are essential.

3.5. Comparison of the Present Results to Those for Other Binary Mixtures. From this study on the basis of the analysis of the concentration dependence of the Raman spectra, it is concluded that acetic acid molecules exist as their microphases in the protic solvents in the region of $\chi_A \geq 0.001$ and as the monomeric forms in the aprotic polar solvents with low electron-donating power in $0.001 \leq \chi_A \leq 0.006$. This means that phase separations at molecular levels occur in binary solutions of acetic acid and the protic solvents (water and alcohol) even in the low acetic acid concentration region, while homogeneously mixed states at molecular levels occur in binary solutions of acetic acid and the aprotic polar solvents (nitriles and ethers) when the mole fraction of acetic acid is smaller than $\chi_A \leq 0.006$.

The question that should be discussed next is whether the above mixing rules at molecular levels can be applied to other binary mixtures or not. In the case of water−acetnitrile mixtures, several studies have been performed to understand their structures.[5,47−49,56,57] Jamroz et al. have obtained quantitative IR spectroscopic data of diluted HDO molecules in CH_3CN-H_2O with ca. 8% HDO.[48] From observation of the constant position and the sharp shape of the OD stretching band at water mole fractions lower than 0.04, they suggested that only water monomers are present in this concentration range. X-ray diffraction measurements on water−acetonitrile binary solutions have also suggested that water−water hydrogen-bonded networks almost disappear at water mole fractions lower than 0.25.[5] NMR spectra of water−acetonitrile and water−acetone mixtures have been interpreted as indicating that a water molecule is associated with the aprotic polar solvents at low water concentrations.[57] From IR spectroscopic studies, methanol has also been considered to exist as its monomeric form in acetonitrile at methanol molar fractions lower than 0.01.[58,59] In ethanol−water mixtures, on the other hand, the mass spectrometric analyses of clusters isolated from liquid droplets have suggested that ethanol−ethanol association is highly preferable even in a diluted aqueous solution with an ethanol mole fraction of 0.02.[60,61] Ultrasonic absorption spectra of mixtures of water with ethanol, propanol isomers, and all isomers of butanol have suggested the existence of alcohol−alcohol associates at alcohol molar fractions higher than 0.05.[62]

As a consequence, from comparison between the previous and the present results, the mixing rules at molecular levels may be proposed as follows: protic−protic binary mixtures do not easily become homogeneously mixed states even when the mixing ratio is large, while homogeneously mixed states at molecular levels preferentially occur in protic−aprotic polar binary mixtures at low concentrations of the protic solvent. The above empirical rules may be interpreted as suggesting that, for the solvent molecules in protic−protic binary mixtures, formation of associated states consisting of the same solvent molecules is more favorable than breaking in hydrogen-bonded networks formed by the other molecules. In this study, we cannot determine the detailed mechanisms governing mixture states at molecular levels. However, it can be said that dimer formation with the cyclic configuration in Figure 9 is one of the vital factors governing the nature of mixture states at molecular levels.

Acknowledgment. This work has been supported by a Grant-in-Aid to T.N. (Grant No. 11740337) from the Ministry of Education, Science, Sports, and Culture in Japan.

References and Notes

(1) Bernal, J. D.; Fowler, R. H. *J. Chem. Phys.* **1933**, *1*, 515.
(2) Ludwig, R.; Weinhold, F.; Farrar, T. C. *J. Chem. Phys.* **1995**, *102*, 5118.

(3) Matsumoto, M.; Nishi, N.; Furusawa, T.; Saita, M.; Takamuku, T.; Yamagami, M.; Yamaguchi, T. *Bull. Chem. Soc. Jpn.* **1995**, *68*, 1775.
(4) Laenen, R.; Rauscher, C. *J. Chem. Phys.* **1997**, *107*, 9759.
(5) Takamuku, T.; Tabata, M.; Yamaguchi, A.; Nishimoto, J.; Kumamoto, M.; Wakita, H.; Yamaguchi, T. *J. Phys. Chem. B* **1998**, *102*, 8880.
(6) Karle, J.; Brockway, L. O. *J. Am. Chem. Soc.* **1944**, *66*, 574.
(7) Derissen, J. L. *J. Mol. Struct.* **1971**, *7*, 67.
(8) Chao, J.; Zwolinski, B. J. *J. Phys. Chem. Ref. Data* **1978**, *7*, 363.
(9) Almenningen, A.; Bastiansen, O.; Motzfeldt, T. *Acta Chem. Scand.* **1969**, *23*, 2848.
(10) Derissen, J. L. *J. Mol. Struct.* **1971**, *7*, 81.
(11) Jones, R. E.; Templeton, D. H. *Acta Crystallogr.* **1958**, *11*, 484.
(12) Nahringbauer, I. *Acta Chem. Scand.* **1970**, *24*, 453.
(13) Jönsson, P.-G. *Acta Crystallogr.* **1971**, *B27*, 893.
(14) Turi, L.; Dannenberg, J. J. *J. Am. Chem. Soc.* **1994**, *116*, 8714.
(15) Holtzberg, F.; Post, B.; Fankuchen, I. *Acta Crystallogr.* **1953**, *6*, 127.
(16) Strieter, F. J.; Templeton, D. H.; Scheuerman, R. F.; Sass, R. L. *Acta Crystallogr.* **1962**, *15*, 1233.
(17) Kanters, J. A.; Kroon, J. *Acta Crystallogr.* **1972**, *B28*, 1946.
(18) Leiserowitz, L. *Acta Crystallogr.* **1976**, *B32*, 775.
(19) Payne, R. S.; Roberts, R. J.; Rowe, R. C.; Docherty, R. *J. Comput. Chem.* **1998**, *19*, 1.
(20) Bertagnolli, H. *Chem. Phys. Lett.* **1982**, *93*, 287.
(21) Faurskov Nielsen, O.; Lund, P.-A. *J. Chem. Phys.* **1983**, *78*, 652.
(22) Yokoyama, I.; Miwa, Y.; Machida, K. *Bull. Chem. Soc. Jpn.* **1992**, *65*, 746.
(23) Briggs, J. M.; Nguyen, T. B.; Jorgensen, W. L. *J. Phys. Chem.* **1991**, *95*, 3315.
(24) Kosugi, K.; Nakabayashi, T.; Nishi, N. *Chem. Phys. Lett.* **1998**, *291*, 253.
(25) Nakabayashi, T.; Kosugi, K.; Nishi, N. *J. Phys. Chem. A* **1999**, *103*, 8595.
(26) Katchalsky, A.; Eisenberg, H.; Lifson, S. *J. Am. Chem. Soc.* **1951**, *73*, 5889.
(27) Cartwright, D. R.; Monk, C. B. *J. Chem. Soc.* **1955**, 2500.
(28) Nash, G. R.; Monk, C. B. *J. Chem. Soc.* **1957**, 4274.
(29) Suzuki, K.; Taniguchi, Y.; Watanabe, T. *J. Phys. Chem.* **1973**, *77*, 1918.
(30) Ng, J. B.; Shurvell, H. F. *J. Phys. Chem.* **1987**, *91*, 496.
(31) Ng, J. B.; Petelenz, B.; Shurvell, H. F. *Can. J. Chem.* **1988**, *66*, 1912.
(32) Kaatze, U.; Menzel, K.; Pottel, R. *J. Phys. Chem.* **1991**, *95*, 324.
(33) Akiyama, Y.; Wakisaka, A.; Mizukami, F.; Sakaguchi, K. *J. Chem. Soc., Perkin Trans. 2* **1998**, 95.
(34) Nishi, N.; Nakabayashi, T.; Kosugi, K. *J. Phys. Chem. A* **1999**, *103*, 10851.
(35) Wong, M. W.; Frisch, M. J.; Wiberg, K. B. *J. Am. Chem. Soc.* **1991**, *113*, 4776.
(36) Foresman, J. B.; Keith, T. A.; Wiberg, K. B.; Snoonian, J.; Frisch, M. J. *J. Phys. Chem.* **1996**, *100*, 16098.
(37) Nara, M.; Torii, H.; Tasumi, M. *J. Phys. Chem.* **1996**, *100*, 19812.
(38) Torii, H.; Tasumi, M. *J. Raman Spectrosc.* **1998**, *29*, 537.
(39) Sato, H.; Hirata, F.; Kato, S. *J. Chem. Phys.* **1996**, *105*, 1546.
(40) Hirata, F. *Bull. Chem. Soc. Jpn.* **1998**, *71*, 1483.
(41) Nakabayashi, T.; Sato, H.; Hirata, F.; Nishi, N. *J. Phys. Chem. A* **2001**, *105*, 245.
(42) Frisch, M. J.; Trucks, G. W.; Schlegel, H. B.; Scuseria, G. E.; Robb, M. A.; Cheeseman, J. R.; Zakrzewski, V. G.; Montgomery, J. A.; Stratmann, R. E.; Burant, J. C.; Dapprich, S.; Millam, J. M.; Daniels, A. D.; Kudin, K. N.; Strain, M. C.; Farkas, O.; Tomasi, J.; Barone, V.; Cossi, M.; Cammi, R.; Mennucci, B.; Pomelli, C.; Adamo, C.; Clifford, S.; Ochterski, J.; Petersson, G. A.; Ayala, P. Y.; Cui, Q.; Morokuma, K.; Malick, D. K.; Rabuck, A. D.; Raghavachari, K.; Foresman, J. B.; Cioslowski, J.; Ortiz, J. V.; Stefanov, B. B.; Liu, G.; Liashenko, A.; Piskorz, P.; Komaromi, I.; Gomperts, R.; Martin, R. L.; Fox, D. J.; Keith, T.; Al-Laham, M. A.; Peng, C. Y.; Nanayakkara, A.; Gonzalez, C.; Challacombe, M.; Gill, P. M. W.; Johnson, B. G.; Chen, W.; Wong, M. W.; Andres, J. L.; Head-Gordon, M.; Replogle, E. S.; Pople, J. A. *Gaussian 98*; Gaussian, Inc.: Pittsburgh, PA, 1998.
(43) Becke, A. D. *J. Chem. Phys.* **1993**, *98*, 5648.
(44) Lee, C.; Yang, W.; Parr, R. G. *Phys. Rev. B* **1988**, *37*, 785.
(45) Miehlich, B.; Savin, A.; Stoll, H.; Preuss, H. *Chem. Phys. Lett.* **1989**, *157*, 200.
(46) Fawcett, W. R.; Liu, G.; Kessler, T. E. *J. Phys. Chem.* **1993**, *97*, 9293.
(47) Reimers, J. R.; Hall, L. E. *J. Am. Chem. Soc.* **1999**, *121*, 3730.
(48) Jamroz, D.; Stangret, J.; Lindgren, J. *J. Am. Chem. Soc.* **1993**, *115*, 6165.
(49) Bertie, J. E.; Lan, Z. *J. Phys. Chem. B* **1997**, *101*, 4111.
(50) Singh, R. K.; Asthana, B. P.; Singth, P. R.; Chakraborty, T.; Verma, A. L. *J. Raman Spectrosc.* **1998**, *29*, 561.
(51) Nakabayashi, T.; Nishi, N. Unpublished results.
(52) *CRC Handbook of Chemistry and Physics*, 81st ed.; Lide, D. R., Ed.; CRC Press: Boca Raton, FL, 2000.
(53) Gutmann, V. *Coord. Chem. Rev.* **1976**, *18*, 225.
(54) Huggins, C. M.; Pimentel, G. C.; Shoolery, J. N. *J. Phys. Chem.* **1956**, *60*, 1311.
(55) Maciel, G. E.; Traficante, D. D. *J. Am. Chem. Soc.* **1966**, *88*, 220.
(56) Venables, D. S.; Schmuttenmaer, C. A. *J. Chem. Phys.* **2000**, *113*, 11222.
(57) Nakahara, M.; Wakai, C. *Chem. Lett.* **1992**, 809.
(58) Mitra, S. S. *J. Chem. Phys.* **1962**, *36*, 3286.
(59) Farwaneh, S. S.; Yarwood, J.; Cabaco, I.; Besnard, M. *J. Mol. Liq.* **1993**, *56*, 317.
(60) Nishi, N.; Koga, K.; Ohshima, C.; Yamamoto, K.; Nagashima, U.; Nagami, K. *J. Am. Chem. Soc.* **1988**, *110*, 5246.
(61) Nishi, N.; Takahashi, S.; Matsumoto, M.; Tanaka, A.; Muraya, K.; Takamuku, T.; Yamaguchi, T. *J. Phys. Chem.* **1995**, *99*, 462.
(62) Brai, M.; Kaatze, U. *J. Phys. Chem.* **1992**, *96*, 8946.